

Dissecting the Diffusion Process in Linear Graph Convolutional Networks

Yifei Wang¹ Yisen Wang¹ Jiansheng Yang¹ Zhouchen Lin¹

Abstract

Graph Convolutional Networks (GCNs) have attracted more and more attentions in recent years. A typical GCN layer consists of a linear feature propagation step and a nonlinear transformation step. Recent works show that a linear GCN can achieve comparable performance to the original non-linear GCN while being much more computationally efficient. In this paper, we dissect the feature propagation steps of linear GCNs from a perspective of continuous graph diffusion, and analyze why linear GCNs fail to benefit from more propagation steps. Following that, we propose Decoupled Graph Convolution (DGC) that decouples the terminal time and the feature propagation steps, making it more flexible and capable of exploiting a very large number of feature propagation steps. Experiments demonstrate that our proposed DGC improves linear GCNs by a large margin and makes them competitive with many modern variants of non-linear GCNs.

1. Introduction

Recently, Graph Convolutional Networks (GCNs) have successfully extended the powerful representation learning ability of modern Convolutional Neural Networks (CNNs) to the graph data (Kipf & Welling, 2017). A graph convolutional layer typically consists of two stages: linear feature propagation and non-linear feature transformation. Simple Graph Convolution (SGC) (Wu et al., 2019) simplifies GCNs by removing the nonlinearities between GCN layers and collapsing the resulting function into a single linear transformation before a single linear classification layer, which makes it a linear GCN. SGC can achieve comparable performance to canonical GCNs while being much more computationally efficient and using significantly fewer parameters. Besides, as softmax regression with a linear model is a convex problem, SGC is much easier to train as common optimizers are guaranteed to reach the global optimum. Thus, we mainly focus on linear GCNs in this paper.

¹Peking University, Beijing, China. Correspondence to: Yisen Wang <yisen.wang@pku.edu.cn>.

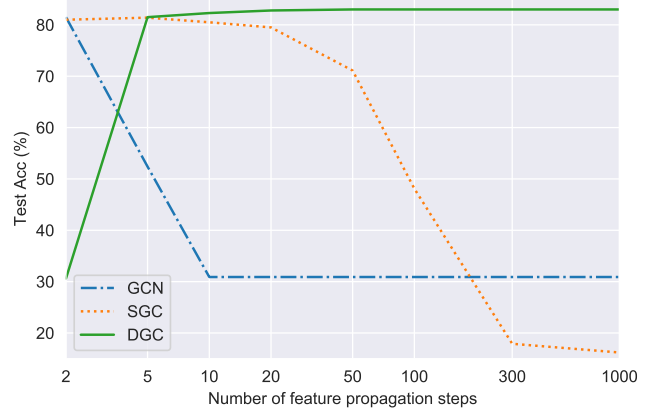


Figure 1. Test accuracy (%) with increasing feature propagation steps on the Cora dataset.

Although being comparable to canonical GCNs, SGC is still much inferior to modern variants of non-linear GCNs. More importantly, it still suffers from a similar issue as non-linear GCNs, that is, more (linear) feature propagation steps K , e.g., $K > 2$, will degrade the performance catastrophically. This issue is widely characterized as the “over-smoothing” phenomenon. Namely, node features will inevitably get smoothed out and lose discriminative ability after too many feature propagation steps (Li et al., 2018).

In this work, through a dissection of the diffusion process of linear GCNs, we characterize a fundamental limitation of SGC. Specifically, we point out that its feature propagation step amounts to a very coarse finite difference with a fixed step size $\Delta t = 1$, which results in a large numerical error. And because the step size is fixed, more feature propagation steps will inevitably lead to a large terminal time $T = K \cdot \Delta t \rightarrow \infty$ that over-smooths the node features.

To address these issues, we propose Decoupled Graph Convolution (DGC) by decoupling the terminal time T and propagation steps K . In particular, we can flexibly choose a continuous terminal time T for the optimal tradeoff between under-smoothing and over-smoothing, and then fix the terminal time while adopting more propagation steps K . In this way, different from SGC that over-smooths with more propagation steps, our proposed DGC can obtain a more fine-grained finite difference approximation with more propagation steps, which contributes to the final performance both theoretically and empirically (a preview result is shown in Figure 1). Extensive experiments show that DGC (as a

linear GCN) improves over SGC significantly and obtains state-of-the-art results that are comparable to many modern variants of non-linear GCNs. Our main contributions are summarized as follows:

- We investigate SGC by dissecting its diffusion process from a continuous perspective, and discuss why it cannot benefit from more propagation steps.
- From the above analysis, we propose Decoupled Graph Convolution (DGC) that decouples the terminal time T and the propagation steps K , which enables us to choose a continuous terminal time flexibly while benefiting from more propagation steps.
- We provide theoretical discussions and comparisons of linear GCNs in terms of their asymptotic, numerical and risk properties from a continuous perspective.

Our experiments show that a properly designed linear GCN (i.e., DGC) can outperform canonical GCNs significantly and obtain state-of-the-art (SOTA) results among linear GCNs. Its performance is even close to that of SOTA non-linear GCNs, thus can serve as a strong baseline for future studies on GCNs.

2. Related Work

2.1. Graph Neural Networks

Graph convolutional networks. To deal with non-Euclidean graph data, GCNs (Kipf & Welling, 2017) are proposed for direct convolution operation over graph, and have drawn interests from various domains. Note that GCN is firstly introduced as a first order approximation of the spectral convolution approach, but soon it becomes popular as a general message passing algorithm in the spatial domain. Many variants have been proposed to improve its performance, such as GraphSAGE (Hamilton et al., 2017) and GAT (Veličković et al., 2018).

Continuous graph neural networks. Deep CNNs, particularly ResNet (He et al., 2016), have been widely interpreted from a continuous perspective that ResNet can be regarded as Euler discretization of Neural ODEs (Lu et al., 2018; Chen et al., 2018b). This viewpoint has also been borrowed to understand and improve GCNs. GDEs (Poli et al., 2019) directly extends GCNs to its Neural ODE counterpart. CGNN (Xhonneux et al., 2020) instead devises a GCN variant inspired by a different continuous diffusion. Our method is also inspired by this connection between discrete and continuous graph diffusion process, but alternatively, we focus on the numerical gap between them and characterize how it affects the final performance. We illustrate the benefit of this connection by showing that decoupling the terminal time T and the finite difference steps K can indeed boost canonical (linear) GCNs by a large margin.

Linear GCNs. SGC (Wu et al., 2019) simplifies and separates the two stages of GCNs: feature propagation and (non-linear) feature transformation. It finds that utilizing only a simple logistic regression after feature propagation (removing the non-linearities), which makes it a linear GCN, can obtain comparable performance to canonical GCNs. PairNorm (Zhao & Akoglu, 2020) proposes a distance regularization to alleviate the over-smoothing problem of SGC. Our work is in the same direction but further tackle over-smoothing by decoupling the terminal time T and feature propagation steps K from a continuous perspective. As a result, we show that linear models can be promoted to have much better performance than SGC and show competitive performance to SOTA non-linear GCN variants.

2.2. Over-smoothing Problem

GCNs face a fundamental problem compared to standard CNNs, i.e., the over-smoothing phenomenon. Li et al. (2018) offers a theoretical characterization of over-smoothing based on linear feature propagation. After that, many researchers have tried to incorporate effective regularization mechanisms in CNNs to alleviate over-smoothing. DropEdge (Rong et al., 2019) applies dropout to graph edges and find it enables training GCNs with more layers. DeepGCNs (Li et al., 2019) shows that residual/dense connection and dilated convolution can make GCNs go as deep as CNNs, although increased depth does not help a lot. PairNorm (Zhao & Akoglu, 2020) regularizes the feature distance to be close to that of the input, where the accuracy will not fail catastrophically but still decrease with more layers.

Our dissection of linear GCNs suggests a different understanding of the over-smoothing problem. As discussed in Section 6, we believe over-smoothing is an inevitable phenomenon of (canonical) GCNs, and we can only find a terminal time for an optimal tradeoff between under-smoothing and over-smoothing. Consequently, we should not expect that more GCN layers can bring more profit if the terminal time goes to infinity. Instead, to alleviate over-smoothing, we should control the terminal time when we adopt more layers. Only at this time can we benefit from the numerical precision with more propagation steps.

3. Preliminary

We make a brief review of SGC (Wu et al., 2019) in the context of semi-supervised node classification task.

3.1. Notations

Define a graph as $\mathcal{G} = (\mathcal{V}, \mathbf{A})$, where \mathcal{V} denotes the vertex set consisting of n nodes $\{v_1, \dots, v_n\}$, and $\mathbf{A} \in \mathbb{R}^{n \times n}$ is a (typically symmetric and sparse) adjacency matrix where a_{ij} denotes the edge weight between node v_i and v_j and a missing edge is denoted as $a_{ij} = 0$. We then define the degree matrix $\mathbf{D} = \text{diag}(d_1, \dots, d_n)$ of \mathbf{A} as a

diagonal matrix whose i -th diagonal entry represents the row sum $d_i = \sum_j a_{ij}$. Each node v_i is represented by a d -dimensional feature vector $\mathbf{x}_i \in \mathbb{R}^d$. A collection of these features $[\mathbf{x}_1, \dots, \mathbf{x}_n]$ constitutes the feature matrix $\mathbf{X} \in \mathbb{R}^{n \times d}$. Each node belongs to one out of C classes, denoted by a C -dimensional one-hot vector $\mathbf{y}_i \in \{0, 1\}^C$. Only a subset of nodes $\mathcal{V}_l \subset \mathcal{V}$ are labeled and we want to predict the labels of the rest unlabeled nodes $\mathcal{V}_u = \mathcal{V} \setminus \mathcal{V}_l$.

3.2. Simple Graph Convolution (SGC)

Simple Graph Convolution (SGC) (Wu et al., 2019) points out that the feature propagation step is the essential ingredient of GCNs and shows that we can obtain comparable results with the following simplified GCN,

$$\hat{\mathbf{Y}}_{\text{SGC}} = \text{softmax}(\mathbf{S}_{\text{SA}}^K \mathbf{X} \Theta), \quad (1)$$

which pre-processes the node features \mathbf{X} with K linear feature propagation steps, and then applies a linear classifier layer with parameter Θ , as described below.

Feature propagation. At this step, each feature \mathbf{x}_i is computed by aggregating features in its local neighborhood,

$$\mathbf{x}_i^{(k)} \leftarrow \frac{1}{d_i + 1} \mathbf{x}_i^{(k-1)} + \sum_{j=1}^n \frac{a_{ij}}{\sqrt{(d_i + 1)(d_j + 1)}} \mathbf{x}_j^{(k-1)}. \quad (2)$$

This operation can be done in parallel over the whole graph, for which we can express as

$$\mathbf{X}^{(k)} \leftarrow \mathbf{S}_{\text{SA}} \mathbf{X}^{(k-1)}, \quad (3)$$

where $\mathbf{S}_{\text{SA}} \in \mathbb{R}^{d \times d}$ refers to the Symmetrically normalized Augmented adjacency matrix:

$$\mathbf{S}_{\text{SA}} = \tilde{\mathbf{D}}^{-\frac{1}{2}} \tilde{\mathbf{A}} \tilde{\mathbf{D}}^{-\frac{1}{2}}, \quad (4)$$

where $\tilde{\mathbf{A}} = \mathbf{A} + \mathbf{I}$ is the augmented adjacency matrix with self-loop and $\tilde{\mathbf{D}}$ is the degree matrix of $\tilde{\mathbf{A}}$. This step exploits local graph structure to smooth out the noise in each node.

Linear classifier. At last, SGC applies multinomial logistic regression (a.k.a. softmax regression) with parameter Θ to predict the node labels $\hat{\mathbf{Y}}_{\text{SGC}}$ from the node features of the last propagation step $\mathbf{X}^{(K)}$:

$$\hat{\mathbf{Y}}_{\text{SGC}} = \text{softmax}(\mathbf{X}^{(K)} \Theta). \quad (5)$$

Because both the feature propagation and classification ($\mathbf{X}^{(K)} \Theta$) steps are linear, SGC is essentially a linear version of GCNs that only relies on linear features extracted from the input. As SGC has decoupled the feature propagation and transformation steps, we can pre-process the feature matrix $\mathbf{X}^{(K)}$ to accelerate the training of the linear classifier. In this way, linear GCNs can be much faster than non-linear GCNs. For example, SGC has demonstrated $28 \times$ acceleration over GCN and $415 \times$ acceleration over GAT.

4. Dissecting Linear GCNs

In this section, we investigate the limitations of current linear GCNs and show how we can improve its performance from a continuous perspective.

A key insight of our work is that the linear feature propagation steps of SGC,

$$\mathbf{X}^{(K)} = \mathbf{S}_{\text{SA}}^K \mathbf{X}, \quad (6)$$

can be seen as a numerical discretization of the corresponding continuous graph diffusion equation:

$$\begin{cases} \frac{d\mathbf{X}_t}{dt} = -\mathbf{L}_{\text{SA}} \mathbf{X}_t, \\ \mathbf{X}_0 = \mathbf{X}, \end{cases} \quad (7)$$

with a finite difference interval of time $\Delta t = 1$ and terminal time $T = K$, where

$$\mathbf{L}_{\text{SA}} = \tilde{\mathbf{D}}^{-\frac{1}{2}} (\tilde{\mathbf{D}} - \tilde{\mathbf{A}}) \tilde{\mathbf{D}}^{-\frac{1}{2}} = \mathbf{I} - \mathbf{S}_{\text{SA}} \quad (8)$$

is the Symmetrically normalized Augmented graph Laplacian, which is symmetric and positive semi-definite.

In the following, we will show that SGC is a coarse finite difference. When applying Euler discretization to Eqn. (7) with an interval Δt , we have

$$\begin{aligned} \mathbf{X}_{t+\Delta t} &= \mathbf{X}_t - \Delta t \tilde{\mathbf{L}}_{\text{SA}} \mathbf{X}_t \\ &= \mathbf{X}_t - \Delta t (\mathbf{I} - \mathbf{S}_{\text{SA}}) \mathbf{X}_t \\ &= [(1 - \Delta t) \mathbf{I} + \Delta t \mathbf{S}_{\text{SA}}] \mathbf{X}_t \\ &\triangleq \mathbf{S}_{\text{SA}}^{(\Delta t)} \mathbf{X}_t, \end{aligned} \quad (9)$$

where $\mathbf{S}_{\text{SA}}^{(\Delta t)} \triangleq (1 - \Delta t) \mathbf{I} + \Delta t \mathbf{S}_{\text{SA}}$ denotes the corresponding feature propagation matrix. If we keep involving the ODE until a terminal time $T = K \cdot \Delta t$, we will get the following final feature matrix:

$$\mathbf{X}_T = [\mathbf{S}_{\text{SA}}^{(\Delta t)}]^K \mathbf{X}. \quad (10)$$

Comparing it to the propagation rule in Eqn. (6), we can see that SGC amounts to the Euler discretization with a very large step size $\Delta t = 1$, where the diffusion matrix reduces to the SGC diffusion matrix \mathbf{S}_{SA} :

$$\mathbf{S}_{\text{SA}}^{(\Delta t)} \Big|_{\Delta t=1} = (1 - 1) \mathbf{I} + \mathbf{S}_{\text{SA}} = \mathbf{S}_{\text{SA}} \quad (11)$$

and the final node features become equivalent:

$$\mathbf{X}_T \Big|_{\Delta t=1} = \mathbf{X}_K = \mathbf{X}^{(K)} = \mathbf{S}_{\text{SA}}^K \mathbf{X}. \quad (12)$$

From this continuous perspective, we can identify the fundamental limitations of SGC, as well as its non-linear counterpart GCNs. On the one hand, they take a very large step size $\Delta t = 1$ in the numerical approximation, which

will result in a large numerical error that largely degrades their estimation precision. On the other hand, as the step size $\Delta t = 1$ is always fixed, a large number of propagation steps K will always amount to a very large terminal time $T = K \cdot \Delta t \rightarrow \infty$. As a result, more depth will inevitably lead to over-smoothing because the node features will become homogeneous at the equilibrium of the diffusion equation in Eqn. (7) as $T \rightarrow \infty$.

5. The Proposed Method

In this section, we introduce our proposed Decoupled Graph Convolution that overcomes the above limitations of SGC.

5.1. Decoupled Graph Convolution

To overcome the above issue of SGC, we need to resolve the coupling between propagation steps K and terminal time T to enable a flexible tradeoff between under-smoothing and over-smoothing and a more fine-grained numerical integration scheme. In particular, we need to rethink the role of propagation steps (network depth for non-linear linear models) K in the over-smoothing problem. If we insist on using a fixed time interval $\Delta t = 1$, more propagation steps (a deeper GCN) will inevitably lead to over-smoothing. As the equilibrium is intrinsic to the diffusion dynamics, we suspect that regularization techniques can alleviate to some degree but cannot fully resolve this fundamental issue.

Thus, we take the terminal time T and the propagation steps K as two free hyper-parameters, instead of enforcing $T = K$. In this way, the two parameters can play different roles and cooperate together to attain better results. Specifically, we can flexibly choose T to tradeoff between under-smoothing and over-smoothing to find a sweet spot for each dataset. Given an optimal terminal time T , we can also flexibly increase the propagation steps K for better numerical precision with $\Delta t = T/K \rightarrow 0$ as $K \rightarrow \infty$. In practice, a moderate number of steps is sufficient to attain the best classification accuracy, hence we can also choose a minimal K among the best for higher computation efficiency.

In this way, we propose our Decoupled Graph Convolution (DGC) as a decoupled version of SGC,

$$\hat{\mathbf{Y}}_{\text{DGC}} = \text{softmax} \left(\left[\mathbf{S}_{\text{SA}}^{(T/K)} \right]^K \mathbf{X} \Theta \right). \quad (13)$$

Specifically, with a predefined terminal time T , we first perform K steps of feature propagation with step size $\Delta t = T/K$ and diffusion matrix $\mathbf{S}_{\text{SA}}^{(T/K)}$:

$$\mathbf{X}_T = \left[\mathbf{S}_{\text{SA}}^{(T/K)} \right]^K \mathbf{X}, \quad (14)$$

and apply logistic regression to the final representation \mathbf{X}_T :

$$\hat{\mathbf{Y}}_{\text{DGC}} = \text{softmax} (\mathbf{X}_T \Theta). \quad (15)$$

5.2. Discussions on Self-loop

Note that the DGC diffusion matrix

$$\mathbf{S}_{\text{SA}}^{(\Delta t)} = (1 - \Delta t) \mathbf{I} + \Delta t \mathbf{S}_{\text{SA}} \quad (16)$$

naturally incorporates the self-loop \mathbf{I} into the diffusion process. The step size Δt serves as a weight parameter for feature aggregation that flexibly tradeoffs between the node itself (by the self-loop matrix \mathbf{I}) and its neighborhood (by the adjacency matrix $\tilde{\mathbf{A}}$). A small step size Δt (or equivalently more steps K with a given T) means more weight on the self-loop term, while a large step size will aggressively aggregate more information from the neighborhood.

Based on the above analysis, we can alternatively remove the self-loop from the augmented adjacency matrix $\tilde{\mathbf{A}} = \mathbf{A} + \mathbf{I}$. The self-loop is heuristically introduced to incorporate information from the node itself and to prevent numerical instability with more steps K , named the *renormalization trick* (Kipf & Welling, 2017). While in our DGC, with the terminal time T fixed, increasing K would not lead to the numerical issues. We name the resulting model as DGC-sym with propagation matrix

$$\mathbf{S}_{\text{sym}}^{(\Delta t)} = (1 - \Delta t) \mathbf{I} + \Delta t \mathbf{S}_{\text{sym}}, \quad (17)$$

where $\mathbf{S}_{\text{sym}} = \mathbf{D}^{-\frac{1}{2}} \mathbf{A} \mathbf{D}^{-\frac{1}{2}}$ is the symmetrically normalized propagation matrix. It is easy to see that the corresponding continuous diffusion is the graph heat equation

$$\begin{cases} \frac{d\mathbf{X}_t}{dt} = -\mathbf{L}_{\text{sym}} \mathbf{X}_t, \\ \mathbf{X}_0 = \mathbf{X}, \end{cases} \quad (18)$$

where $\mathbf{L}_{\text{sym}} = \mathbf{I} - \mathbf{D}^{-\frac{1}{2}} \mathbf{A} \mathbf{D}^{-\frac{1}{2}}$ is the canonical symmetrically normalized graph Laplacian (Defferrard et al., 2016). Experiments show that this diffusion yield comparable performance to the self-augmented version, while it typically requires more steps K to obtain the best results. In other words, the added self-loop bias explicitly preserves the unique node information and achieves faster convergence to the desired representation for node classification.

6. Theoretical Analysis

In this section, we provide a characterization of the theoretical properties of canonical linear GCNs as well as our proposed DGC.

6.1. Asymptotic Analysis

Previous works that characterize the over-smoothing phenomenon of linear GCNs focus on the discrete regime (Li et al., 2018), which requires certain assumptions on the graph structure. In our work, we instead adopt the continuous view of linear GCNs and provide a clearer characterization of the dynamics of graph propagation relying only on the spectrum of graph Laplacian.

For the general graph heat equation with Laplacian \mathbf{L} ,

$$\begin{cases} \frac{d\mathbf{X}_t}{dt} = -\mathbf{L}\mathbf{X}_t, \\ \mathbf{X}_0 = \mathbf{X}, \end{cases} \quad (19)$$

it admits the following closed-form solution,

$$\mathbf{X}_t = e^{-t\mathbf{L}}\mathbf{X}_0, \quad (20)$$

where $\mathbf{H}_t \triangleq e^{-t\mathbf{L}}$ is often referred to as the *heat kernel* in the spectral graph literature (Chung & Graham, 1997), and the matrix exponential is defined based on Taylor expansion:

$$e^{\mathbf{X}} = \sum_{k=0}^{\infty} \frac{1}{k!} \mathbf{X}^k, \text{ where } \mathbf{X}^0 \triangleq \mathbf{I}. \quad (21)$$

Asymptotics of heat kernel. To understand the behavior of \mathbf{X}_t as $t \rightarrow \infty$, we need to study the asymptotic property of the heat kernel \mathbf{H}_t . We note that both \mathbf{L}_{SA} and \mathbf{L}_{sym} are symmetric and positive semi-definite, thus we can perform eigen-decomposition of the graph Laplacian:

$$\mathbf{L} = \mathbf{U}\mathbf{\Lambda}\mathbf{U}^\top, \quad (22)$$

where $\mathbf{U} \in \mathbb{R}^{n \times n}$ is an orthogonal matrix whose columns are the eigenvectors of \mathbf{L} , and $\mathbf{\Lambda} \in \mathbb{R}^{n \times n}$ is a diagonal matrix whose entries are the eigenvalues of \mathbf{L} . Because \mathbf{L} is symmetric and positive semi-definite, all eigenvalues are non-negative real numbers, i.e., $\lambda_i \geq 0, i = 1, \dots, n$. With the eigen-decomposition of Laplacian, we have the following asymptotic properties of heat kernel.

Theorem 1. *The heat kernel $\mathbf{H}_t = e^{-t\mathbf{L}}$ admits the following eigen-decomposition,*

$$\mathbf{H}_t = \mathbf{U} \begin{pmatrix} e^{-\lambda_1 t} & 0 & \dots & 0 \\ 0 & e^{-\lambda_2 t} & \dots & 0 \\ \vdots & \vdots & \ddots & \vdots \\ 0 & 0 & \dots & e^{-\lambda_n t} \end{pmatrix} \mathbf{U}^\top. \quad (23)$$

As a result, with $\lambda_i \geq 0$, we have

$$\lim_{t \rightarrow \infty} e^{-\lambda_i t} = \begin{cases} 0, & \text{if } \lambda_i > 0 \\ 1, & \text{if } \lambda_i = 0 \end{cases}, i = 1, \dots, n. \quad (24)$$

Proof. See Appendix. \square

Therefore, given a non-trivial graph, e.g., $\mathbf{A} \neq \mathbf{I}$, the graph Laplacian would have positive eigenvalues and the corresponding spectral features would be smoothed out to zero as $t \rightarrow \infty$. If the graph Laplacian is positive definite, i.e. $\lambda_i > 0, \forall i$, we would have

$$\lim_{t \rightarrow \infty} \mathbf{X}_t = \lim_{t \rightarrow \infty} \mathbf{H}_t \mathbf{X}_0 = \mathbf{0}, \quad (25)$$

where $\mathbf{0}$ denotes the matrix with all zero entries. In other words, all node features are smoothed out and lose discriminative ability.

Comparing SGC and DGC. In SGC, with a fixed step size $\Delta t = 1$, more propagation $K \rightarrow \infty$ means $T \rightarrow \infty$, which inevitably leads to the above over-smoothing issue. Instead, in our DGC, with a fixed finite terminal time $T < \infty$, increasing the number of step $K = T/\Delta t \rightarrow \infty$ amounts to decreasing the time interval Δt , which would not result in over-smoothing.

6.2. Numerical Analysis

In this part, we further provide a non-asymptotic analysis of the numerical error with our numerical integration methods. Specifically, given a terminal time T , we have the closed form solution to the continuous heat equation as

$$\mathbf{X}_T = e^{-T\mathbf{L}}\mathbf{X}_0 = \left[\sum_{k=1}^{\infty} \frac{T^k}{k!} (-\mathbf{L})^k \right] \mathbf{X}_0, \quad (26)$$

while the numerical solution given by the forward Euler method with K steps is

$$\hat{\mathbf{X}}_T^{(K)} = \left(\mathbf{I} - \frac{T}{K}\mathbf{L} \right)^K \mathbf{X}_0. \quad (27)$$

Denote the numerical error between the analytic solution and the numerical solution as

$$\mathbf{e}_T^{(K)} = \mathbf{X}_T - \hat{\mathbf{X}}_T^{(K)}. \quad (28)$$

The following theorem shows that the numerical error is $O(1/K)$, which goes to zero as $K \rightarrow \infty$.

Theorem 2. *For the general initial value problem in Eqn. (40) with any finite terminal time T , the numerical error of the forward Euler method in Eqn. (41) with K propagation steps can be upper bounded by*

$$\|\mathbf{e}_T^{(K)}\| \leq \frac{T\|\mathbf{L}\|\|\mathbf{X}_0\|}{2K} \left(e^{T\|\mathbf{L}\|} - 1 \right). \quad (29)$$

Proof. See Appendix. \square

Comparing SGC and DGC. In SGC, we have $T = K$, thus the numerical error can be very large, which will keep increasing with more steps as $T = K \rightarrow \infty$. While in DGC, with a fixed terminal time T , increasing the feature propagation steps will shrink the numerical error and improve the final estimate, which can explain why DGC can benefit from depth and will not suffer from over-smoothing.

Effect of Laplacian. In Theorem 2, the numerical error is positively correlated to the norm of the Laplacian matrix. As the two Laplacian matrices considered in our work, \mathbf{L}_{SA} and \mathbf{L}_{sym} , both have spectral range within $[0, 2]$, $\|\mathbf{L}\|$ is bounded. We also note that the spectral range of \mathbf{L}_{SA} is strictly smaller than \mathbf{L}_{sym} (Wu et al., 2019), thus the corresponding problem would have smaller numerical error with the same propagation steps, as empirically verified by our experiments.

6.3. Risk Analysis

In the above discussion, we have shown that our DGC yields better numerical precision in the approximation of the continuous diffusion. Here, we further show that it indeed corresponds to smaller learning risk under certain model assumptions. For simplicity, we consider the following node regression problem:

$$\mathbf{Y} = \mathbf{X}_c \mathbf{W}_c + \sigma_y \varepsilon_y, \quad \varepsilon_y \sim \mathcal{N}(\mathbf{0}, \mathbf{I}); \quad (30)$$

$$\hat{\mathbf{X}}_0 = \mathbf{X}_c + \sigma_x \varepsilon_x, \quad \varepsilon_x \sim \mathcal{N}(\mathbf{0}, \mathbf{I}); \quad (31)$$

$$\frac{d\hat{\mathbf{X}}_t}{dt} = \mathbf{L}\hat{\mathbf{X}}_t, \quad \hat{\mathbf{X}}_{T^*} = e^{t\mathbf{L}}\hat{\mathbf{X}}_0. \quad (32)$$

The classification problem has similar results by taking the convex logsoftmax operator into consideration. Eqn. (55) describes the ground truth generation process of target label \mathbf{Y} from the clean (unobserved) node features \mathbf{X}_c with weight matrix \mathbf{W}_c and additive independent Gaussian noise ε_y . Eqn. (56) & (57) describe the data corruption process: we firstly add independent noise to each node, and then further corrupt each node feature by an inverse graph heat equation that enhances the noise by graph diffusion for time T^* . At last, we collect the corrupted data $\hat{\mathbf{X}} = \mathbf{X}_{T^*}$ as our observed data.

Our goal is to learn the weight matrix \mathbf{W} from the corrupted data $(\hat{\mathbf{X}}, \mathbf{Y})$ with the following linear GCN with K propagation steps and terminal time \hat{T} ,

$$\hat{\mathbf{Y}} = \mathbf{X}_{\hat{T}}^{(K)} \mathbf{W}, \quad \mathbf{X}_{\hat{T}}^{(K)} = [\mathbf{S}^{(\hat{T}/K)}]^K \mathbf{X}_0, \quad \mathbf{X}_0 = \hat{\mathbf{X}}. \quad (33)$$

Theorem 3. Denote the population risk of the ground truth regression problem with weight \mathbf{W} as

$$R(\mathbf{W}) = \mathbb{E}_{p(\mathbf{X}_c, \mathbf{Y})} \|\mathbf{Y} - \mathbf{X}_c \mathbf{W}\|^2. \quad (34)$$

and that of the corrupted regression problem as

$$\hat{R}(\mathbf{W}) = \mathbb{E}_{p(\hat{\mathbf{X}}, \mathbf{Y})} \left\| \mathbf{Y} - [\mathbf{S}^{(\hat{T}/K)}]^K \hat{\mathbf{X}} \mathbf{W} \right\|^2. \quad (35)$$

Supposing that $\mathbb{E}\|\mathbf{X}_c\|^2 = M < \infty$, we have the following upper bound on the latter risk:

$$\begin{aligned} \hat{R}(\mathbf{W}) \leq & R(\mathbf{W}) + \|\mathbf{W}\|^2 \left[\sigma_x^2 + (M + \sigma_x^2) \left\| e^{T^* \mathbf{L}} \right\|^2 \right. \\ & \left. \cdot \left(\left\| e^{-T^* \mathbf{L}} - e^{-\hat{T} \mathbf{L}} \right\|^2 \right) + \mathbb{E} \left\| \mathbf{e}_{T^*}^{(K)} \right\|^2 \right]. \end{aligned} \quad (36)$$

Proof. See Appendix. \square

Comparing SGC and DGC. From the theorem, we can see that the population risk gap can be minimized by finding the optimal terminal time such that $\hat{T} = T^*$, and minimizing the numerical error $\mathbf{e}_{T^*}^{(K)}$ (Eqn. (42)) at the optimal terminal

Table 1. Dataset statistics of the citation networks (Sen et al., 2008) and Reddit (Hamilton et al., 2017).

Dataset	# Nodes	# Edges	Train/Dev/Test Nodes
Cora	2,708	5,429	140/500/1,000
Citeseer	3,327	4,732	120/500/1,000
Pubmed	19,717	44,338	60/500/1,000
Reddit	233K	11.6M	152K/24K/55K

time, which corresponds to the two failure modes of SGC: 1) SGC will introduce diffusion error if the ground truth terminal time T^* is not an integer; and 2) SGC also leads to a large numerical error with a large step size $\Delta t = 1$. Our DGC does not suffer from these problems as it can flexibly choose a continuous terminal time T and reduce the numerical error by applying more propagation steps K .

7. Experiments

In this section, we evaluate DGC on a collection of benchmark datasets of node classification tasks and compare it with modern variants of linear and non-linear GCNs. Afterwards, we conduct a comprehensive analysis on DGC.

7.1. Performance on Benchmark Datasets

Datasets. Following previous practice (Kipf & Welling, 2017; Wu et al., 2019), we evaluate our DGC on the semi-supervised node classification tasks. One is the citation network task (Sen et al., 2008), which includes three different datasets, Cora, Citeseer, and Pubmed. We also conduct experiments on a much larger graph, the Reddit dataset (Hamilton et al., 2017), for inductive prediction of the Reddit community structure. Note that we use the standard dataset splits as in Kipf & Welling (2017). Dataset statistics are summarized in Table 1.

Training hyper-parameters. We train our DGC with the same hyper-parameters as SGC (Wu et al., 2019). Specifically, on the citation networks, we train DGC for 100 epochs using Adam (Kingma & Ba, 2015) with learning rate 0.2. For weight decay, as in SGC, we tune this hyperparameter on each dataset using hyperopt (Bergstra et al., 2015) for 10,000 trails. On the Reddit dataset, we train DGC with L-BFGS (Liu & Nocedal, 1989) using no regularization for 2 steps. We evaluate DGC for the inductive task (Reddit) following Chen et al. (2018a): we firstly train DGC on a subgraph comprising only training nodes, and then test the model with the original graph and learned parameters.

Baselines. We compare our DGC against several representative non-linear and linear methods for learning from graph. For non-linear GCNs, we include both spectral methods (Yang et al., 2016; Kipf & Welling, 2017; Xu et al., 2019; 2020), spatial methods (Veličković et al., 2018; Veličković et al., 2019; Gao & Ji, 2019; Zhang & Meng, 2019), together

Table 2. Test accuracy (%) averaged over 10 runs on three citation networks, Cora, Citeseer and Pubmed, with the standard data split. For previous methods, we report the numbers from previous literature and also report variance if available.

Type	Method	Cora	Citeseer	Pubmed
Non-linear	Planetoid (Yang et al., 2016)	75.7	64.7	77.2
	GCN (Kipf & Welling, 2017)	81.5	70.3	79.0
	GAT (Velićković et al., 2018)	83.0 \pm 0.7	72.5 \pm 0.7	79.0 \pm 0.3
	GWWN (Xu et al., 2019)	82.8	71.7	79.1
	DGI (Velickovic et al., 2019)	82.3 \pm 0.6	71.8 \pm 0.7	76.8 \pm 0.6
	Graph U-Nets (Gao & Ji, 2019)	84.4 \pm 0.6	73.2 \pm 0.5	79.6 \pm 0.2
	GCDE (Poli et al., 2019)	83.8 \pm 0.5	72.5 \pm 0.5	79.9 \pm 0.3
	GraphHeat (Xu et al., 2020)	83.7	72.5	80.5
	Graph-BERT (Zhang et al., 2020)	84.3	71.2	79.3
Linear	Label Propagation (Zhu et al., 2003)	45.3	68.0	63.0
	DeepWalk (Perozzi et al., 2014)	70.7 \pm 0.6	51.4 \pm 0.5	76.8 \pm 0.6
	SGC (Wu et al., 2019)	81.0 \pm 0.0	71.9 \pm 0.1	78.9 \pm 0.0
	SGC-PairNorm (Zhao & Akoglu, 2020)	81.1	70.6	78.2
	DGC (ours)	83.0 \pm 0.0	73.3 \pm 0.1	80.2 \pm 0.0

Table 3. Test accuracy (%) averaged over 10 runs on a large scale dataset Reddit with the standard data split. OOM: out of memory. GraphSAGE: the method by Hamilton et al. (2017). RandDGI: DGI (Velickovic et al., 2019) with randomly initialized encoder.

Type	Method	Acc
Non-linear	GCN (Kipf & Welling, 2017)	OOM
	GraphSAGE-GCN	93.0
	GraphSAGE-mean	95.0
	GraphSAGE-LSTM	95.4
	FastGCN (Chen et al., 2018a)	93.7
	SIGN (Rossi et al., 2020)	96.8
	GraphSAINT (Zeng et al., 2020)	97.0
Linear	RandDGI (Velickovic et al., 2019)	93.3
	SGC (Wu et al., 2019)	94.9
	DGC (ours)	95.3

with a continuous model GCDE (Poli et al., 2019). For linear methods, we present the results of Label Propagation (Zhu et al., 2003), DeepWalk (Perozzi et al., 2014), and the linear GCN SGC (Wu et al., 2019) as well as its regularized version SGC-PairNorm (Zhao & Akoglu, 2020).

DGC v.s. previous linear methods. We list the results on the citation networks in Table 2, and the results on the large scale dataset Reddit in Table 3. We can see that with the decoupled terminal time T and propagation steps K , we can further push the limit of linear GCNs and improve over SGC significantly.

Linear v.s. non-linear models. We can see that our linear DGC improves a lot over canonical GCNs (Kipf & Welling, 2017) on all datasets, as shown in Tables 2 and 3. Furthermore, DGC is comparable to, and sometimes outperforms,

many non-linear variants of GCNs developed recently. We also note that the gap between linear and non-linear models is a little larger on large graphs like Reddit, which suggests that there is still room for improving linear models by incorporating more advanced techniques.

DGC v.s. non-linear continuous GCNs. In Table 2, comparing DGC with GCDE (Poli et al., 2019) that applies non-linear Neural ODE on graphs, we can see that our DGC achieves comparable accuracy with linear dynamics.

Stability. Another advantage of DGC is that it is more numerically stable because it is a convex model and the optimization methods are typically guaranteed to reach the global optimum. As shown in Table 2, the results of DGC have much smaller variance compared to non-linear GCNs.

7.2. Comprehensive Analysis on DGC

We further study the different aspects of our proposed DGC in terms of the Laplacian matrix, numerical scheme, computation time and terminal time. We adopt the same experimental setup as the previous subsection unless specified.

Laplacian. From Figure 2 (left), we can see with decoupled terminal time T and propagation steps K , neither of the two Laplacian matrices lead to over-smoothing with more propagation steps. Instead, they both benefit from larger K . Comparing the two Laplacians, we can see that the augmented Laplacian \mathbf{S}_{SA} obtains higher test accuracy than the canonical Laplacian \mathbf{L}_{sym} and requires fewer propagation steps K to obtain the best result. Intuitively, the added self-loop in \mathbf{S}_{SA} helps preserve the node information during the propagation. From a spectral perspective (Section 6.2), \mathbf{L}_{SA} will yield smaller numerical error because it has a smaller spectral range than \mathbf{L}_{sym} .

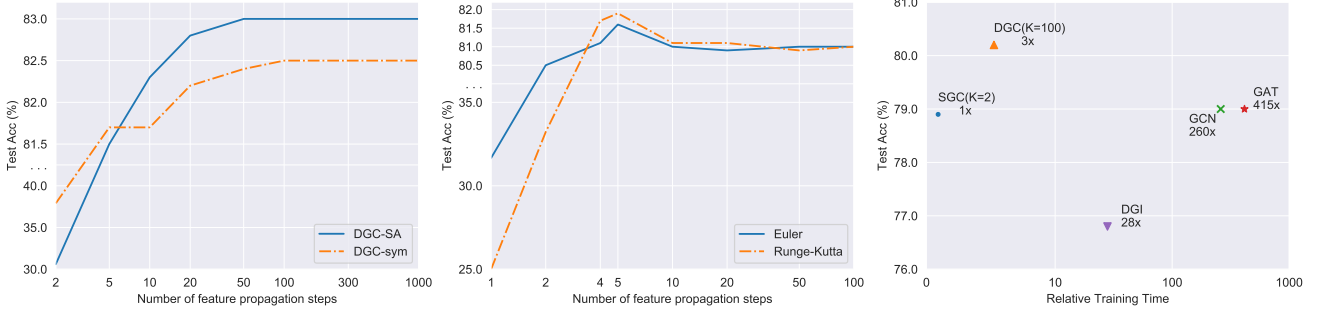


Figure 2. Algorithmic analysis of our proposed DGC. Left: test accuracy (%) comparison of different Laplacian matrices with increasing steps K and optimal terminal time (fixed) on the Cora dataset. Middle: test accuracy (%) comparison of different numerical schemes with increasing steps K , Laplacian \mathbf{S}_{SA} and optimal terminal time T (fixed) on the Cora dataset. Right: relative total training time comparison of different GCNs on the Pubmed dataset. We note that SGC is equivalent to DGC with $K = T = 2$ and Laplacian \mathbf{S}_{SA} . For DGC, we measure a typical setting with 100 steps.

Numerical scheme. Alternatively, we can apply higher-order finite difference methods to achieve better numerical precision, at the cost of more function evaluation at intermediate points. One of the classical methods is the fourth-order Runge-Kutta (RK) method. In Figure 2 (middle), we compare the test accuracy of different numerical methods. We find that the Runge-Kutta method demonstrates better accuracy than the Euler method with a moderate K . Nevertheless, as K increases, the difference gradually vanishes. Therefore, we take the Euler method in our DGC for its simplicity and efficiency.

Computation time. In Figure 2 (right), we show that DGC is slightly more computationally expensive ($3\times$) than SGC but with higher performance. Even so, it is still much faster than non-linear GCNs ($> 100\times$).

Terminal time T . In Table 4, we compare the test accuracy with different terminal time T . We show that there exists a sweet spot of terminal time that achieves the optimal tradeoff between under-smoothing and over-smoothing. For example, we find that $T = 3.5$ performs better than $T = 2$ of SGC with $K = 2$ propagation steps on Cora dataset. In Table 5, we list the best terminal time and number of steps found by hyperopt (Bergstra et al., 2015) on two large graph datasets. We can see that T is almost consistent on each dataset, suggesting that the optimal terminal time is an intrinsic property of the dataset. We can also see that the augmented Laplacian indeed requires fewer steps to obtain the optimal performance.

8. Conclusions

In this paper, we have proposed Decoupled Graph Convolution (DGC), which improves significantly over previous linear GCNs through decoupling the terminal time and feature propagation steps from a continuous perspective. Experiments show that our DGC is competitive with many modern variants of non-linear GCNs while being much more computationally efficient with much fewer parameters to learn.

Table 4. Test accuracy (%) with Laplacian \mathbf{S}_{sym} and different terminal time T on the Cora dataset. For a fair comparison, we take a fixed number of feature propagation steps ($K = 100$) in each setting of DGC. NA: not applicable.

T	1	2	3	3.5	4	6	10
SGC	69.6	80.5	79.2	NA	81.0	80.5	79.2
DGC	78.0	81.0	82.0	82.5	81.8	81.1	79.4

Table 5. Test accuracy (%) with the optimal terminal time T and propagation steps K on the Pubmed and Reddit datasets.

Dataset	Laplacian	T	K	Acc (%)
Pubmed	\mathbf{S}_{SA}	5.1	4	80.2
	\mathbf{S}_{sym}	5.2	580	79.2
Reddit	\mathbf{S}_{SA}	3.8	31	95.1
	\mathbf{S}_{sym}	3.8	67	95.3

Our findings suggest that, unfortunately, current GCN variants still have not shown significant advantages over a properly designed linear GCN. We believe that this would attract the attention of the community to reconsider the actual representation ability of current nonlinear GCNs and propose new alternatives that can truly benefit from nonlinear architectures.

References

- Bergstra, J., Komer, B., Eliasmith, C., Yamins, D., and Cox, D. D. Hyperopt: a python library for model selection and hyperparameter optimization. *Computational Science & Discovery*, 8(1):014008, 2015.
- Chen, J., Ma, T., and Xiao, C. FastGCN: fast learning with graph convolutional networks via importance sampling. *ICLR*, 2018a.
- Chen, R. T., Rubanova, Y., Bettencourt, J., and Duvenaud,

- D. K. Neural ordinary differential equations. *NeurIPS*, 2018b.
- Chung, F. R. and Graham, F. C. *Spectral graph theory*. Number 92. American Mathematical Soc., 1997.
- Defferrard, M., Bresson, X., and Vandergheynst, P. Convolutional neural networks on graphs with fast localized spectral filtering. *NeurIPS*, 2016.
- Gao, H. and Ji, S. Graph U-nets. *ICML*, 2019.
- Hamilton, W., Ying, Z., and Leskovec, J. Inductive representation learning on large graphs. *NeurIPS*, 2017.
- He, K., Zhang, X., Ren, S., and Sun, J. Deep residual learning for image recognition. *CVPR*, 2016.
- Kingma, D. P. and Ba, J. Adam: A method for stochastic optimization. *ICLR*, 2015.
- Kipf, T. N. and Welling, M. Semi-supervised classification with graph convolutional networks. *ICLR*, 2017.
- Li, G., Muller, M., Thabet, A., and Ghanem, B. DeepGCNs: Can gcns go as deep as cnns? *CVPR*, 2019.
- Li, Q., Han, Z., and Wu, X.-M. Deeper insights into graph convolutional networks for semi-supervised learning. *AAAI*, 2018.
- Liu, D. C. and Nocedal, J. On the limited memory BFGS method for large scale optimization. *Mathematical programming*, 45(1):503–528, 1989.
- Lu, Y., Zhong, A., Li, Q., and Dong, B. Beyond finite layer neural networks: Bridging deep architectures and numerical differential equations. *ICML*, 2018.
- Perozzi, B., Al-Rfou, R., and Skiena, S. DeepWalk: Online learning of social representations. *SIGKDD*, 2014.
- Poli, M., Massaroli, S., Park, J., Yamashita, A., Asama, H., and Park, J. Graph neural ordinary differential equations. *arXiv preprint arXiv:1911.07532*, 2019.
- Rong, Y., Huang, W., Xu, T., and Huang, J. DropEdge: Towards deep graph convolutional networks on node classification. *ILCR*, 2019.
- Rossi, E., Frasca, F., Chamberlain, B., Eynard, D., Bronstein, M., and Monti, F. SIGN: Scalable inception graph neural networks. *arXiv preprint arXiv:2004.11198*, 2020.
- Sen, P., Namata, G., Bilgic, M., Getoor, L., Galligher, B., and Eliassi-Rad, T. Collective classification in network data. *AI magazine*, 29(3):93–93, 2008.
- Veličković, P., Cucurull, G., Casanova, A., Romero, A., Lio, P., and Bengio, Y. Graph attention networks. *ICLR*, 2018.
- Velickovic, P., Fedus, W., Hamilton, W. L., Liò, P., Bengio, Y., and Hjelm, R. D. Deep graph infomax. *ICLR*, 2019.
- Wu, F., Zhang, T., Souza Jr, A. H. d., Fifty, C., Yu, T., and Weinberger, K. Q. Simplifying graph convolutional networks. *ICML*, 2019.
- Xhonneux, L.-P., Qu, M., and Tang, J. Continuous graph neural networks. *ICML*, 2020.
- Xu, B., Shen, H., Cao, Q., Qiu, Y., and Cheng, X. Graph wavelet neural network. *ICLR*, 2019.
- Xu, B., Shen, H., Cao, Q., Cen, K., and Cheng, X. Graph convolutional networks using heat kernel for semi-supervised learning. *arXiv preprint arXiv:2007.16002*, 2020.
- Yang, Z., Cohen, W., and Salakhudinov, R. Revisiting semi-supervised learning with graph embeddings. *ICML*, 2016.
- Zeng, H., Zhou, H., Srivastava, A., Kannan, R., and Prasanna, V. GraphSAINT: Graph sampling based inductive learning method. *ICLR*, 2020.
- Zhang, J. and Meng, L. GResNet: Graph residual network for reviving deep gnns from suspended animation. *arXiv preprint arXiv:1909.05729*, 2019.
- Zhang, J., Zhang, H., Xia, C., and Sun, L. Graph-BERT: Only attention is needed for learning graph representations. *arXiv preprint arXiv:2001.05140*, 2020.
- Zhao, L. and Akoglu, L. PairNorm: Tackling oversmoothing in gnns. *ICLR*, 2020.
- Zhu, X., Ghahramani, Z., and Lafferty, J. D. Semi-supervised learning using gaussian fields and harmonic functions. *ICML*, 2003.

A. Proof of Theorem 1

Theorem 1. The heat kernel $\mathbf{H}_t = e^{-t\mathbf{L}}$ admits the following eigen-decomposition,

$$\mathbf{H}_t = \mathbf{U} \begin{pmatrix} e^{-\lambda_1 t} & 0 & \cdots & 0 \\ 0 & e^{-\lambda_2 t} & \cdots & 0 \\ \vdots & \vdots & \ddots & \vdots \\ 0 & 0 & \cdots & e^{-\lambda_n t} \end{pmatrix} \mathbf{U}^\top. \quad (37)$$

As a result, with $\lambda_i \geq 0$, we have

$$\lim_{t \rightarrow \infty} e^{-\lambda_i t} = \begin{cases} 0, & \text{if } \lambda_i > 0 \\ 1, & \text{if } \lambda_i = 0 \end{cases}, \quad i = 1, \dots, n. \quad (38)$$

Proof. With the eigen-decomposition of the Laplacian $\mathbf{L} = \mathbf{U}\mathbf{\Lambda}\mathbf{U}^\top$, the heat kernel can be written equivalently as

$$\mathbf{H}_t = e^{-t\mathbf{L}} = \sum_{k=0}^{\infty} \frac{t^k}{k!} (-\mathbf{L})^k = \sum_{k=0}^{\infty} \frac{t^k}{k!} [\mathbf{U}(-\mathbf{\Lambda})\mathbf{U}^\top]^k = \mathbf{U} \left[\sum_{k=0}^{\infty} \frac{t^k}{k!} (-\mathbf{\Lambda})^k \right] \mathbf{U}^\top = \mathbf{U} e^{-t\mathbf{\Lambda}} \mathbf{U}^\top, \quad (39)$$

which corresponds to the eigen-decomposition of the heat kernel with eigen-vectors in the orthogonal matrix \mathbf{U} and eigen-values in the diagonal matrix $e^{-t\mathbf{\Lambda}}$. Now it is easy to see the limit behavior of the heat kernel as $t \rightarrow \infty$ from the spectral domain. \square

B. Proof of Theorem 2

Theorem 2. For the general initial value problem

$$\begin{cases} \frac{d\mathbf{X}_t}{dt} = -\mathbf{L}\mathbf{X}_t, \\ \mathbf{X}_0 = \mathbf{X}, \end{cases} \quad (40)$$

with any finite terminal time T , the numerical error of the forward Euler method

$$\hat{\mathbf{X}}_T^{(K)} = \left(\mathbf{I} - \frac{T}{K} \mathbf{L} \right)^K \mathbf{X}_0. \quad (41)$$

with K propagation steps can be upper bounded by

$$\|\mathbf{e}_T^{(K)}\| \leq \frac{T\|\mathbf{L}\|\|\mathbf{X}_0\|}{2K} \left(e^{T\|\mathbf{L}\|} - 1 \right). \quad (42)$$

Proof. Consider a general Euler forward scheme for our initial problem

$$\hat{\mathbf{X}}^{(k+1)} = \hat{\mathbf{X}}^{(k)} - h\mathbf{L}\hat{\mathbf{X}}_t, \quad k = 0, 1, \dots, K-1, \quad \mathbf{X}^{(0)} = \mathbf{X}, \quad (43)$$

where $\hat{\mathbf{X}}^{(k)}$ denotes the approximated \mathbf{X} at step k , h denotes the step size and the terminal time $T = Kh$. We denote the global error at step k as

$$\mathbf{e}_k = \mathbf{X}^{(k)} - \hat{\mathbf{X}}^{(k)}, \quad (44)$$

and the truncation error of the Euler forward finite difference (Eqn. (43)) at step k as

$$\mathbf{T}^{(k)} = \frac{\mathbf{X}^{(k+1)} - \mathbf{X}^{(k)}}{h} + \mathbf{L}\mathbf{X}^{(k)}. \quad (45)$$

We continue by noting that Eqn. (45) can be written equivalently as

$$\mathbf{X}^{(k+1)} = \mathbf{X}^{(k)} + h \left(\mathbf{T}^{(k)} - \mathbf{L}\mathbf{X}^{(k)} \right). \quad (46)$$

Taking the difference of Eqn. (46) and (43), we have

$$\mathbf{e}^{(k+1)} = (1 - h\mathbf{L})\mathbf{e}^{(k)} + h\mathbf{T}^{(k)}, \quad (47)$$

whose norm can be upper bounded as

$$\|\mathbf{e}^{(k+1)}\| \leq (1 + h\|\mathbf{L}\|) \|\mathbf{e}^{(k)}\| + h\|\mathbf{T}^{(k)}\|. \quad (48)$$

Let $M = \max_{0 \leq k \leq K-1} \|\mathbf{T}^{(k)}\|$ be the upper bound on global truncation error, we have

$$\|\mathbf{e}^{(k+1)}\| \leq (1 + h\|\mathbf{L}\|) \|\mathbf{e}^{(k)}\| + hM. \quad (49)$$

By induction, and noting that $1 + h\|\mathbf{L}\| \leq e^{h\|\mathbf{L}\|}$ and $\mathbf{e}^{(0)} = \mathbf{X}^{(0)} - \hat{\mathbf{X}}^{(0)} = \mathbf{0}$, we have

$$\|\mathbf{e}^{(K)}\| \leq \frac{M}{\|\mathbf{L}\|} [(1 + h\|\mathbf{L}\|)^n - 1] \leq \frac{M}{\|\mathbf{L}\|} (e^{Kh\|\mathbf{L}\|} - 1). \quad (50)$$

Now we note that $\frac{d\mathbf{X}^{(k)}}{dt} = -\mathbf{L}\mathbf{X}^{(k)}$ and applying Taylor's theorem, there exists $\delta \in [nh, (k+1)h]$ such that the truncation error $\mathbf{T}^{(k)}$ in Eqn. (45) follows

$$\mathbf{T}^{(k)} = \frac{1}{2h} \mathbf{L}^2 \mathbf{X}_\delta. \quad (51)$$

Thus the truncation error can be bounded by

$$\|\mathbf{T}^{(k)}\| = \frac{1}{2h} \|\mathbf{L}\|^2 \|\mathbf{X}_\delta\| \leq \frac{1}{2h} \|\mathbf{L}\|^2 \|\mathbf{X}_0\|, \quad (52)$$

because

$$\|\mathbf{X}_\delta\| = \|e^{-\delta\mathbf{L}} \mathbf{X}_0\| \leq \|\mathbf{X}_0\|, \quad \forall \delta \geq 0. \quad (53)$$

Together with the fact $T = Kh$, we have

$$\|\mathbf{e}^{(K)}\| \leq \frac{\|\mathbf{L}\|^2 \|\mathbf{X}_0\|}{2h\|\mathbf{L}\|} (e^{Kh\|\mathbf{L}\|} - 1) = \frac{T\|\mathbf{L}\| \|\mathbf{X}_0\|}{2K} (e^{T\|\mathbf{L}\|} - 1), \quad (54)$$

which completes the proof. \square

C. Proof of Theorem 3

For the data generation process

$$\mathbf{Y} = \mathbf{X}_c \mathbf{W}_c + \sigma_y \varepsilon_y, \quad \varepsilon_y \sim \mathcal{N}(\mathbf{0}, \mathbf{I}); \quad (55)$$

$$\hat{\mathbf{X}}_0 = \mathbf{X}_c + \sigma_x \varepsilon_x, \quad \varepsilon_x \sim \mathcal{N}(\mathbf{0}, \mathbf{I}); \quad (56)$$

$$\frac{d\hat{\mathbf{X}}_t}{dt} = \mathbf{L}\hat{\mathbf{X}}_t, \quad \hat{\mathbf{X}}_{T^*} = e^{t\mathbf{L}} \hat{\mathbf{X}}_0, \quad (57)$$

and observed data $\hat{\mathbf{X}} = \hat{\mathbf{X}}_{T^*}$, we have the following bound on its population risks.

Theorem 3. Denote the population risk of the ground truth regression problem with weight \mathbf{W} as

$$R(\mathbf{W}) = \mathbb{E}_{p(\mathbf{X}_c, \mathbf{Y})} \|\mathbf{Y} - \mathbf{X}_c \mathbf{W}\|^2. \quad (58)$$

and that of the corrupted regression problem as

$$\hat{R}(\mathbf{W}) = \mathbb{E}_{p(\hat{\mathbf{X}}, \mathbf{Y})} \left\| \mathbf{Y} - \left[\mathbf{S}^{(\hat{T}/K)} \right]^K \hat{\mathbf{X}} \mathbf{W} \right\|^2. \quad (59)$$

Supposing that $\mathbb{E}\|\mathbf{X}_c\|^2 = M < \infty$, we have the following upper bound on the latter risk:

$$\hat{R}(\mathbf{W}) \leq R(\mathbf{W}) + \|\mathbf{W}\|^2 \left[\sigma_x^2 + (M + \sigma_x^2) \left\| e^{T^* \mathbf{L}} \right\|^2 \cdot \left(\left\| e^{-T^* \mathbf{L}} - e^{-\hat{T} \mathbf{L}} \right\|^2 \right) + \mathbb{E} \left\| \mathbf{e}_{T^*}^{(K)} \right\|^2 \right]. \quad (60)$$

Proof. Considering $\hat{\mathbf{X}}_0 = e^{-T^* \mathbf{L}} \hat{\mathbf{X}}$, given the fact that

$$\mathbb{E}_{p(\hat{\mathbf{X}}, \mathbf{Y})} \|\hat{\mathbf{X}}_0\|^2 = \mathbb{E}_{p(\hat{\mathbf{X}}, \mathbf{Y})} \|\mathbf{X}_c + \sigma_x \boldsymbol{\varepsilon}_x\|^2 \leq \mathbb{E}_{p(\hat{\mathbf{X}}, \mathbf{Y})} \|\mathbf{X}_c\|^2 + \mathbb{E}_{p(\hat{\mathbf{X}}, \mathbf{Y})} \|\sigma_x \boldsymbol{\varepsilon}_x\|^2 \leq M + \sigma_x^2,$$

we can decompose the corrupted population risk as follows

$$\begin{aligned} \hat{R}(\mathbf{W}) &= \mathbb{E}_{p(\hat{\mathbf{X}}, \mathbf{Y})} \left\| \mathbf{Y} - \left[\mathbf{S}^{(\hat{T}/K)} \right]^K \hat{\mathbf{X}} \mathbf{W} \right\|^2 \\ &= \mathbb{E}_{p(\hat{\mathbf{X}}, \mathbf{Y})} \left\| \mathbf{Y} - \hat{\mathbf{X}}_0 \mathbf{W} + \hat{\mathbf{X}}_0 \mathbf{W} - \left[\mathbf{S}^{(\hat{T}/K)} \right]^K \hat{\mathbf{X}} \mathbf{W} \right\|^2 \\ &= \mathbb{E}_{p(\hat{\mathbf{X}}, \mathbf{Y})} \left\| \mathbf{Y} - (\mathbf{X}_c + \sigma_x \boldsymbol{\varepsilon}_x) \mathbf{W} + \left(e^{-T^* \mathbf{L}} - \left[\mathbf{S}^{(\hat{T}/K)} \right]^K \right) \hat{\mathbf{X}} \mathbf{W} \right\|^2 \\ &\leq \mathbb{E}_{p(\hat{\mathbf{X}}, \mathbf{Y})} \left\| \mathbf{Y} - \mathbf{X}_c \mathbf{W} \right\|^2 + \|\mathbf{W}\|^2 \sigma_x^2 + \|\mathbf{W}\|^2 \mathbb{E}_{p(\hat{\mathbf{X}}, \mathbf{Y})} \left\| \left(\left[e^{-\hat{T} \mathbf{L}} - \mathbf{S}^{(\hat{T}/K)} \right]^K \right) \hat{\mathbf{X}} + \left(e^{-T^* \mathbf{L}} - e^{-\hat{T} \mathbf{L}} \right) \hat{\mathbf{X}} \right\|^2 \\ &\leq \mathbb{E}_{p(\hat{\mathbf{X}}, \mathbf{Y})} \left\| \mathbf{Y} - \mathbf{X}_c \mathbf{W} \right\|^2 + \|\mathbf{W}\|^2 \sigma_x^2 + \|\mathbf{W}\|^2 \mathbb{E}_{p(\hat{\mathbf{X}}, \mathbf{Y})} \left\| \mathbf{e}_{\hat{T}}^{(K)} + \left(e^{-T^* \mathbf{L}} - e^{-\hat{T} \mathbf{L}} \right) e^{T^* \mathbf{L}} \hat{\mathbf{X}}_0 \right\|^2 \\ &\leq R(\mathbf{W}) + \|\mathbf{W}\|^2 \left(\sigma_x^2 + \mathbb{E} \left\| \mathbf{e}_{\hat{T}}^{(K)} \right\|^2 + (M + \sigma_x^2) \left\| e^{T^* \mathbf{L}} \right\|^2 \left\| e^{-T^* \mathbf{L}} - e^{-\hat{T} \mathbf{L}} \right\|^2 \right), \end{aligned} \tag{61}$$

which completes the proof. \square